IEEE Access
Multidisciplinary | Rapid Review | Open Access Journal

SPECIAL SECTION ON TUNABLE DEVICES FOR MODERN COMMUNICATIONS: MATERIALS, INTEGRATION, MODELING, AND APPLICATIONS

Received December 18, 2017, accepted January 14, 2018, date of publication January 18, 2018, date of current version March 19, 2018.

Digital Object Identifier 10.1109/ACCESS.2018.2795463

Vanadium Oxide Bandstop Tunable Filter for Ka Frequency Bands Based on a Novel Reconfigurable Spiral Shape Defected Ground Plane CPW

EMANUELE ANDREA CASU[1], ANDREI A. MÜLLER[1], MONTSERRAT FERNÁNDEZ-BOLAÑOS[1], ALESSANDRO FUMAROLA[2], ANNA KRAMMER[3], ANDREAS SCHÜLER[3], AND ADRIAN M. IONESCU[1]

[1]Nanoelectronic Devices Laboratory, École Polytechnique Fédérale de Lausanne, CH-1015 Lausanne, Switzerland
[2]Max Planck Institute of Microstructure Physics, 06120 Halle, Germany
[3]Solar Energy and Building Physics Laboratory, École Polytechnique Fédérale de Lausanne, CH-1015 Lausanne, Switzerland

Corresponding author: Andrei A. Müller (andrei.muller@epfl.ch)

This work was supported in part by the HORIZON2020 PHASE-CHANGE SWITCH Project under Grant 737109, in part by the ERC Advanced Grant Milli-tech of the European Commission under Grant 695459, and in part by the Swiss Federal Office of Energy under Grant 8100072.

ABSTRACT This paper proposes and validates a new principle in coplanar waveguide (CPW) bandstop filter tuning by shortcutting defected ground plane (DGS) inductor shaped spirals to modify the resonant frequency. The tunable filter is fabricated on a high-resistivity silicon substrate based on a CMOS compatible technology using a 1 μm × 10 μm long and 300 nm thick vanadium oxide (VO_2) switch by exploiting its insulator to metal transition. The filter is designed to work in K_a band with tunable central frequencies ranging from 28.2 GHz to 35 GHz. The measured results show a tuning range of more than 19 %, a low insertion loss in the neighboring frequency bands (below 2 dB at 20 GHz and 40 GHz in on/off-states) while a maximum rejection level close to 18 dB in off-state, limited by the no RF-ideal CMOS compatible substrate. The filter has a footprint of only $0.084 \cdot \lambda_0 \times 0.037 \cdot \lambda_0$ (where λ_0 represents the free space wavelength at the highest resonance frequency) thus making it the most compact configuration using CPW DGS structures for the K_a frequency band. In addition, a more compact filter concept based on the Peano space filling curve is introduced to increase the tuning range while minimizing the DGS area.

INDEX TERMS Microwave filters, millimeter wave technology, thin films, vanadium oxide.

I. INTRODUCTION

The recent fast development of the future space communication in the K_a frequency band [1] motivates the research of new tunable components for this frequency range applications, among which tunable bandstop filters [2] play a major role.

Because of its ease of integration, reversible insulator to metal transition (IMT), low transition temperature and fast switching time, the employment of Vanadium Dioxide (VO_2) as a reconfigurable RF material has been recently investigated for a variety of microwave devices [2]–[4] and employed in bandstop filter design in [2] up to 22.5 GHz by means of a defected ground plane design (DGS) [2], [5]. DGS were introduced in 2000 [5] and have since then [6] been extensively used both in microstrip and coplanar waveguide technology (CPW) for microwave filter design at a variety of frequencies [5]–[14].

In CPW technology by embedding a DGS, depending on the shape and substrate properties several tunable bandstop filters [2], [6], [9], [13] and bandstop structures [7], [8] were reported. However only very few K_a frequency band bandstop filters were proposed [2], [11]–[13] and among them even fewer [2], [13] were reconfigurable or fabricated [13]. A summary of the K_a band DGS CPW bandstop filters performances is shown in Table 1, while Table 2 depicts other fabricated K_a CPW bandstop filters performances. Table 1 and Table 2 show the features of these filters in terms of tuning range, tunability (defined as in [2] as $|f_{max} - f_{min}|/f_{max}$ where

TABLE 1. Ka Bandstop filter performances in CPW technology using DGS.

	Frequency (GHz)	Measured	Tunability %	Q_{max}	*IL* 20 GHz/40 GHz (dB)	Size: $(b\times a)/\lambda_0^2$	Max *IL*(dB) Ka band
[2] (Fig. 8)	26.6-30.6	No	13 %	Q_{max} <27	3/1 on-state 2.5/2.8 off-state	0.14×0.04	18.8/16
[11]	~32	Yes	No	Q_{max} =27	1/1	0.05×0.02	~8
[12]	~28	No	No	Q_{max}>30	1/not reported	0.13×0.092	~26
This work	28.27-35.00	Yes	19.2 %	Q_{on}=14 Q_{off}=35	1.9/1 on-state 1.2/2.4 off-state	0.076×0.033	12.8/18.3

TABLE 2. Other recent Microwave CPW fabricated bandstop filter performances.

	Frequency (GHz)	Measured	Tunability %	Size: $(b\times a)/\lambda_0^2$	Max *IL* (dB) (different states)
[13]	35-38	Yes	9 %	0.18×0.123	20.2/18
[9]	1.69-2.16	Yes	22 %	0.13×0.05	30/16

f_{max} stands for the highest frequency and f_{min} for the minimum frequency), maximum insertion loss (*IL*), quality factor Q defined as f_0/B_{3dB} (f_0 where B_{3dB} denotes the bandwidth at 3 dB) and size (defined as in Fig.1 as the area of the defected part $b \times a$ of the transmission line divided by the squared free space wavelength λ_0^2 at the highest resonance frequency tuned).

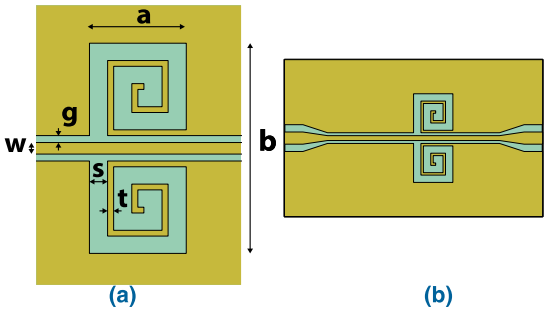

FIGURE 1. (a) Layout of the proposed DGS shape and its area defined as $a \times b$ (area of a rectangle covering the defected shape) with $w = 40$ μm and $g = 24$ μm, $s = 60$ μm, $t = 20$ μm and $a = 320$ μm, (b) including the matching network to a CPW line with $w = 100$ μm central width line and $g = 60$ μm employed for the measurement of the device.

The forms of the reported DGS used in tunable bandstop filters or resonators structures include mainly squares and rectangles [2], [6], square patches [7], [8], a succession of square patches [9] or a succession of squares [10].

From the tuning mechanism viewpoint the fabricated reported bandstop filters employing DGS (considering the entire microwave frequency spectrum) use varactors [7], [9] or PIN diodes [8] for tuning ranges not exceeding 10 GHz and VO_2 [2] for the 19.8-22.5 GHz frequency ranges.

In this paper we introduce to the best of our knowledge a new tuning mechanism for the CPW DGS bandstop filter design by shortcutting the turns of spiral inductors [11], [14] by using a 300 nm × 1 μm × 10 μm VO_2 tuning switch, where the resonant frequency is controlled by the DGS inductor self resonance. In [15] tunable inductors with VO_2 have been proposed with a different switching mechanism and not as DGS.

In terms of normalized size ($b \times a/\lambda_0^2$) the proposed filters occupy around half of the area of the other K_a band tunable reported CPW DGS filters [2] (Table 1) or other bandstop filters employing a DGS form (Table 2) [9], [13].

The fabricated filter has a high tuning range of 19 % while exhibiting lower losses in the K band and at 40 GHz than the CPW DGS measured filters present in literature for the same frequency band [11]. The fabrication is done in CMOS compatible technology and the tuning is achieved by heating the VO_2 film above the IMT temperature (68 °C) causing its conductivity to increase of about three orders of magnitude. The off-state is defined for the VO_2 film in its insulating phase (at 20 °C) with low conductivity while for the on-state the film is in its metallic phase (above the temperature) and thus presents higher conductivity. The maximum *IL* in the on-state is directly influenced by the properties of the used VO_2 film, since the switches are used as series elements (differently from [2] where capacitive switches were proposed).

The paper presents first the design mechanism employing tunable inductors DGS, then it introduces the fabrication process and presents the measurement of the fabricated devices. In the discussion section it introduces a new conceptual layout based on a space filling curve.

II. DESIGN OF FIXED BANDSTOP FILTERS USING SPIRAL DEFECTED GROUND PLANE

A. SIMULATION OF THE FILTER WITHOUT TUNING MECHANISM IN ON-STATE

The design of the spiral DGS follows the principles presented in [11] and [14] for non-reconfigurable bandstop filters. The substrate used is as in [11] a silicon wafer

(with relative dielectric permittivity $\varepsilon_r = 11.7$ and thickness of $h = 525$ μm) passivated with 500 nm SiO_2. The CPW line parameters are presented in Fig. 2. where w denotes the width of the central line while g the distance between the central line and the ground planes ($w = 40$ μm and $g = 24$ μm) . The metallization is a 2000 nm thick aluminum film.

The values for the spiral DGS are chosen in order to get a resonant frequency around 28 GHz while obtaining attenuation levels higher than the ones reported in [11] for the same substrate (and frequency band) and keeping the *IL* below 2 dB in the K band and at 40 GHz.

The attenuation values obtained could be improved by increasing the metal thickness, by using a more conductive metal or by using the improved substrates as presented in [16], but the aim of this work is to focus on the new compact tuning principle while aiming enhanced results compared to [2] and [11] where the same substrate is used.

The physical filter layout values presented in Fig. 1(a) and the final filter layout presented in Fig. 1(b) are obtained using the Ansys HFSS terminal solutions solver. The optimized matching network added in Fig. 1(b) is needed to test the filter employing the measuring equipment used.

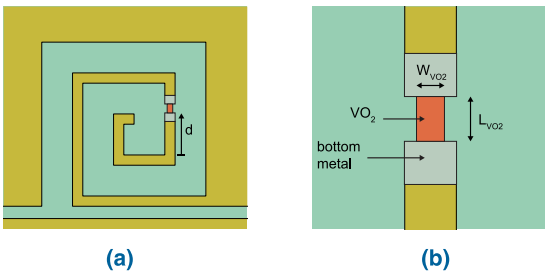

FIGURE 2. (a) VO_2 (orange) interrupting the spiral inductor DGS in the off-state and continuing it in the on-state. (b) Closer view of the VO_2 switch with its geometrical parameters.

The tuning mechanism proposed in this paper consists in cutting a gap in the spiral inductor DGS and adding in it a thin VO_2 layer. The position of the gap changes the resonant frequency of the filter in the "off-state", while its length has an important impact on the filter performances in the on-state. Fig. 2(a) and (b) depict the gap positioning d and the VO_2 integration and geometrical parameters. The results in terms of magnitude of the scattering transmission parameter S_{21} are presented in Fig. 3 considering first the ideal presented in Fig. 1. The obtained values show a 19.8 dB insertion loss at $f_0 = 28.1$ GHz and a quality factor $Q = 28$, similar to the values obtained in [17].

B. SIMULATION OF THE FILTER WITH TUNING MECHANISM IN THE ON-STATE

Fig. 4 shows the performances in the "on-state" of the filter with integrated VO_2 in the gap (Fig. 2.) by considering first different gap lengths. As the length increases from 1 μm to 11 μm the maximum *IL* decreases from around 17.67 dB to 9.4 dB, while the Q of the filters decreases too. Fig. 5 shows the influence of the VO_2 film conductivity in its metallic phase. It can be seen that the use of a low conductive VO_2 film affects the maximum *IL* for fixed geometrical values of the film.

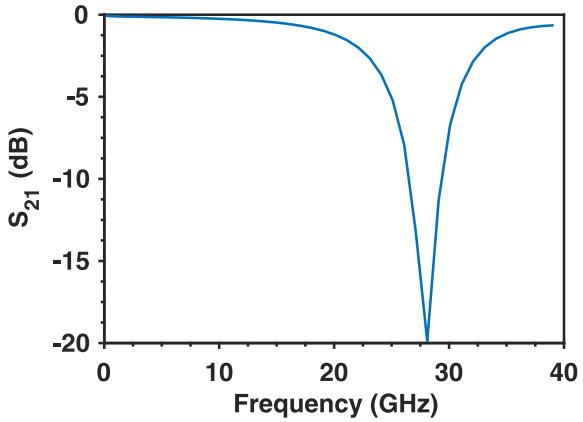

FIGURE 3. Simulated transmission parameter S_{21} magnitude for the structure in Fig. 1(b).

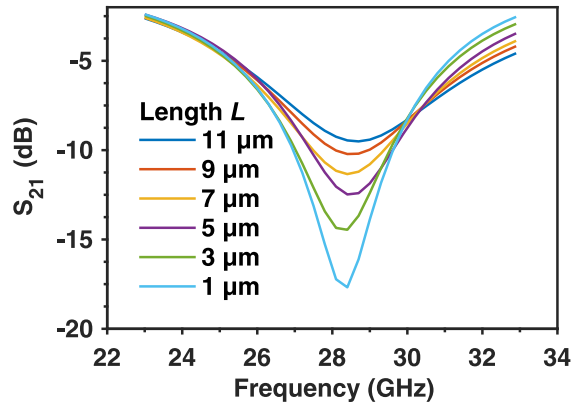

FIGURE 4. Simulated magnitude of the transmission parameter S_{21} for different length of the VO_2 filled gap considering a 30000 S/m conductivity of the chosen thin film, a width of 20 μm and a thickness of 300 nm.

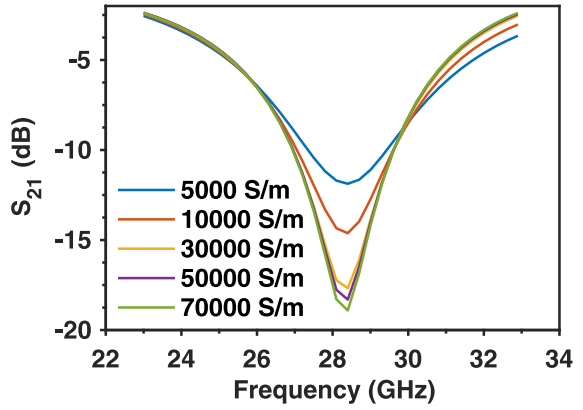

FIGURE 5. Simulated magnitude of the transmission parameter S_{21} for varying conductivity of the VO_2 thin film for a width of 20 μm, a length of 1 μm and a thickness of 300 nm.

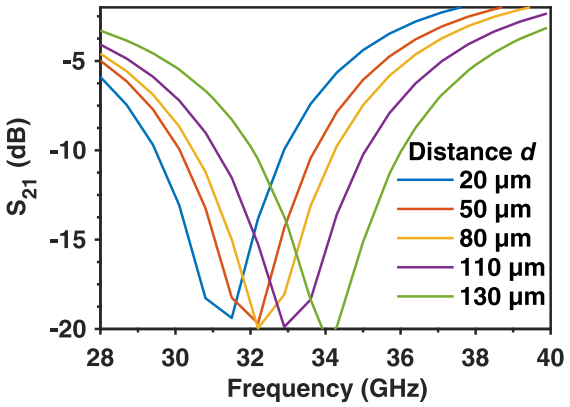

FIGURE 6. Simulated magnitude of the transmission parameter S_{21} for different position d of the VO_2 switch along the spiral (as indicated in Fig. 3) in the off-state.

C. SIMULATION OF THE FILTER WITH TUNING MECHANISM IN THE OFF-STATE

The DGS can be seen like a dual of a spiral inductor which has two spirals short-cutted when the VO_2 is in the non-conductive state (off). The position of the switch along the spiral determines the value of the inductance in the off-state and thus sets the resonant frequency. Fig. 6 shows the effect of changing the value of d (position of the cut along the spiral): the resonance frequency increases as d is increased and the cut is done further away from the reference in Fig. 2 (a). One can see a shift from 28 GHz in the on-state to around 34 GHz in the off-state as d reaches 130 µm. It is worth mentioning that a further displacement of the cut position along the spiral would further increase the tuning range. The results presented in Fig. 6. are based on a VO_2 switch of length of $L_{VO2} = 1$ µm considering a constant relative dielectric permittivity of $\varepsilon_r = 30$ for the thin film.

The final parameters of the fabricated filter are $a = 320$ µm, $d = 130$ µm with a VO_2 switch of length $L_{VO2} = 1$ µm and width $W_{VO2} = 10$ µm.

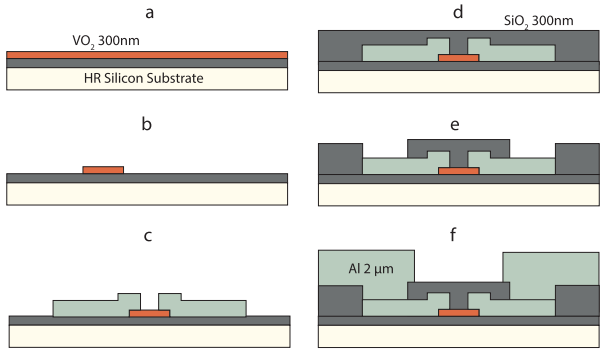

FIGURE 7. Fabrication process of the vanadium oxide tunable band-stop filters. (a) VO_2 sputtering. (b) VO_2 patterning. (c) Ti 20 nm/Al 800 nm Lift-Off. (d) SiO_2 sputtering. (e) VIAS opening. (f) Al sputtering and etching.

III. FABRICATION

The filters were fabricated using standard microelectronics processes starting with a high-resistivity (10000 Ω · cm) 525 µm thick silicon substrate (Fig. 7). A 300 nm thick

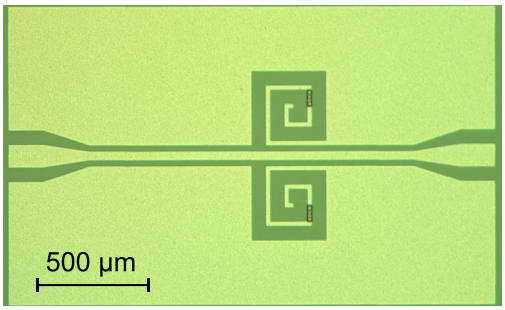

FIGURE 8. Optical image of the fabricated tunable band-stop filter.

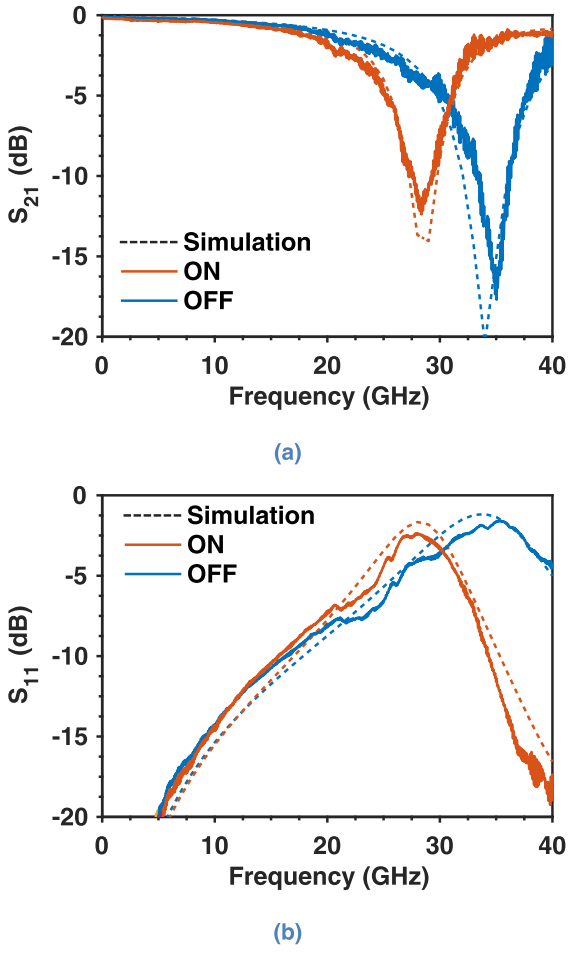

FIGURE 9. Measured magnitudes of the S_{21} (a) and S_{11} (b) parameters at 20 °C (OFF) and at 100 °C (ON) (solid lines) versus simulated with Ansys HFSS for the corresponding conductivity values of the VO_2 film (dotted lines) (The simulations are done for a VO_2 film width of 10 µm, a length of 1 µm and a thickness of 300 nm as fabricated while using a conductivity of 30000 S/m in the On-state).

amorphous silicon layer was deposited to improve radiofrequency performances [16]. The substrate was then passivated with 500 nm SiO_2 deposited by sputtering. The VO_2 film was prepared by reactive magnetron sputtering deposition starting from a Vanadium target [18]. The film was then patterned using photolithography and wet etching. To contact the VO_2 20 nm of Titanium and 800 nm of Aluminum film were subsequently deposited with e-beam evaporation and patterned with lift-off. A 300 nm thick SiO_2 film was then

sputtered. Vias were opened by photolithography and dry etching of SiO_2 to contact the bottom metal and a final 2 μm thick Aluminum top metal layer was deposited to create the CPW. Fig. 8 shows an optical image of fabricated filter.

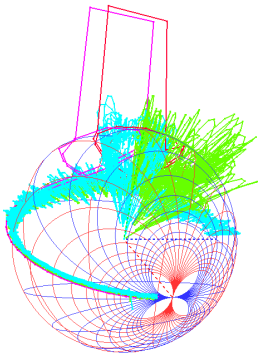

FIGURE 10. Measured group delay in the range 0-40 GHz represented over the S_{21} parameters with the 3D Smith chart [19], [20]. The group delay peaks do not exceed in absolute value 0.27 ns (off measured - green, on measured - cyan, off simulated - red, on simulated - violet).

IV. MEASUREMENTS AND DISCUSSION

Fig. 9 presents the measured magnitude of the S_{21} parameters at 20 °C for the off-state and 100 °C for the on-state (well above the insulator to metal transition temperature of the VO_2 film) and shows good agreement with the simulations. The group delay, shown in Fig. 10 by using [19] and [20], has a flat value in both states presenting measured peak variations below 0.27 ns, slightly larger than the simulated value of 0.25 ns, but similar to the reported values in [17]. It is worth mentioning the almost indistinguishable difference between the simulated complex S_{21} parameters and measured ones in both states (plotted on the surface of the 3D Smith chart)

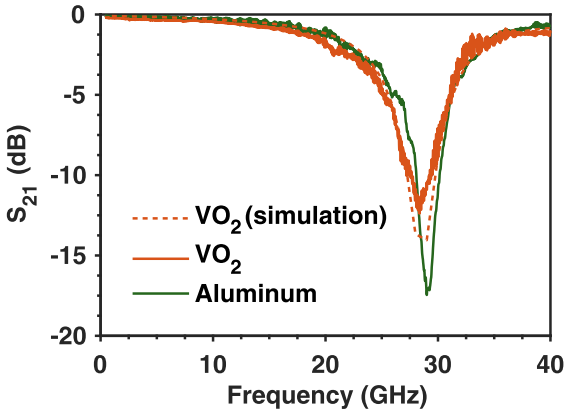

FIGURE 11. Measured magnitude of the S_{21} parameter for a structure with VO_2 switch at 100 °C (ON) (red solid lines), for a structure with Aluminum instead of VO_2 (green) and for the simulated Ansys HFSS for the 30000 S/m conductivity values of the VO_2 film in the on-state (dashed red line).

In order to better understand the *IL* performances in the on-state we fabricated a test device where the VO_2 film is replaced with a metallic strip and we obtained the results in Fig. 11, showing the limitation caused by the thin film non ideal behavior (we used in the simulations a value of 30000 S/m for the expected conductivity). To avoid an excessive quality factor drop below unity as in [15] where the VO_2 was used (in a completely different approach) in spiral inductor design, a very short VO_2 gap (1 μm) was used.

In the off-state the frequency shift could be attributed to the modelling used for the VO_2 permittivity, which changes as the frequency increases [3] and whose exact value is difficult to predict.

Using the same tuning concept, inspired from the Peano space filling curve [21], which was used very recently in other microwave applications [22], we introduce to the best of our knowledge for the first time a Peano DGS for the bandstop filter tuning. The position of the VO_2 switch in this layout allows changing the resonance frequency in various ways (an example being presented in Fig. 12), offering thus a flexible tuning capability. Again the maximum *IL* are limited by the substrate losses, switching losses but the proposed design allows minimizing the area while increasing the tuning range.

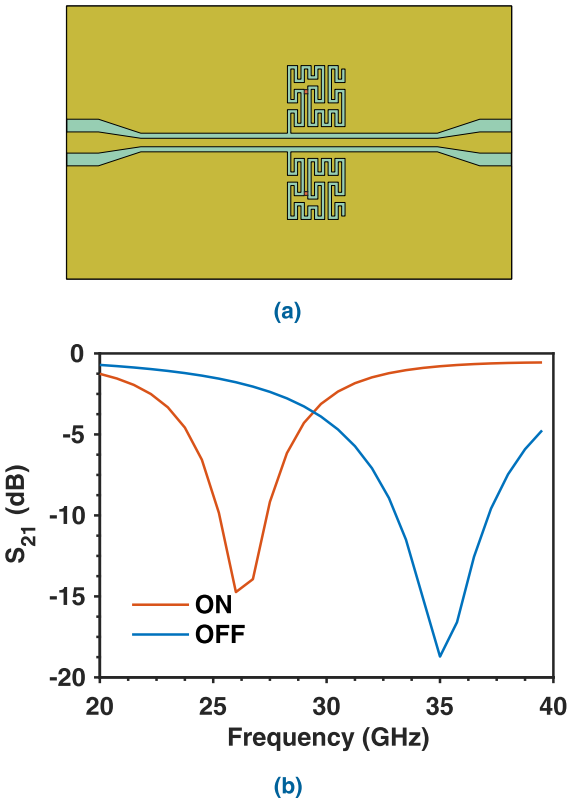

FIGURE 12. (a) Conceptual Peano curve shaped DGS band stop filter (switch position is with red color) filter and (b) corresponding S_{21} parameters magnitudes simulated with Ansys HFSS. Normalized filter size = $b \times a/\lambda_0^2 = 0.08 \times 0.03$.

V. CONCLUSION

We have reported the first VO_2 based K_a band CPW DGS experimental bandstop tunable filter. The filter occupies the smallest area in respect to all other CPW DGS tunable filters

known to the authors in terms of area divided by the square of free space wavelength (defined at the highest tuned resonance frequency) while exhibiting a tunability of 19 %. The use of VO_2 as a contact series switch shows the high dependence of the maximum *IL* obtained at the tuned resonance frequency on the conductivity and length/width of the VO_2 thin film. Even if the on-state performances of the filters are limited by the VO_2 conductivity and by the non-ideal silicon substrate, the tuning defected shape principles introduced may be of further interest for the microwaves community. Last, based on the same tuning principle we introduce a new type of conceptual Peano filter prototype for minimizing the DGS area while adding a potential degree of flexibility in the tuning capabilities.

REFERENCES

[1] NASA Glenn Research Center. *Press release, Ka Band Represents the Future of Satellite Communications*. Accessed: Aug. 2017. [Online]. Available: https://www.nasa.gov/mission_pages/station/research/news/ka_band

[2] W. A. Vitale *et al.*, "Electrothermal actuation of vanadium dioxide for tunable capacitors and microwave filters with integrated microheaters," *Sensors Actuat. A, Phys.*, vol. 241, pp. 245–253, Apr. 2016.

[3] N. Edmond, A. Hendaoui, S. Delprat, M. Chaker, and K. Wu, "Theoretical and experimental investigation of thermo-tunable metal-insulator-vanadium dioxide coplanar waveguide structure," *IEEE Trans. Microw. Theory Techn.*, vol. 65, no. 5, pp. 1443–1455, May 2017.

[4] E. A. Casu *et al.*, "Shunt capacitive switches based on VO_2 metal insulator transition for RF phase shifter applications," in *Proc. ESSDERC*, Leuven, Belgium, Sep. 2017, pp. 232–235.

[5] C. S. Kim, J. S. Park, D. Ahn, and J. B. Lim, "A novel 1-D periodic defected ground structure for planar circuits," *IEEE Microw. Wireless Lett.*, vol. 10, no. 4, pp. 131–133, Apr. 2000.

[6] M. K. Khandelwal, B. K. Kanaujia, and S. Kumar, "Defected ground structure: Fundamentals, analysis, and applications in modern wireless trends," *Hindawi Int. J. Antennas Propag.*, vol. 2017, Feb. 2017, Art. no. 2018527.

[7] A. M. E. Safwat, F. Podevin, P. Ferrari, and A. Vilcot, "Tunable bandstop defected ground structure resonator using reconfigurable dumbbell-shaped coplanar waveguide," *IEEE Trans. Microw. Theory Techn.*, vol. 54, no. 9, pp. 3559–3564, Sep. 2006.

[8] H. B. El-Shaarawy, F. Cocceti, R. Plana, M. El-Said, and E. A. Hashish, "Novel reconfigurable defected ground structure resonator on coplanar waveguide," *IEEE Trans. Microw. Theory Techn.*, vol. 58, no. 11, pp. 3622–3628, Nov. 2010.

[9] J. Wang, H. Ning, and L. Mao, "A compact reconfigurable bandstop resonator using defected ground structure on coplanar waveguide," *IEEE Antennas Wireless Propag. Lett.*, vol. 11, pp. 457–459, Apr. 2012.

[10] A. Chernov, Y. Prokopenko, and G. A. E. Vandenbosch, "Continuously tunable band-stop filter based on coplanar waveguide with defected ground structure," in *Proc. Int. Conf. Electron. Nanotechnol. (ELNANO)*, Apr. 2017, pp. 187–189.

[11] D. Schlieter and R. M. Henderson, "Silicon integrated defected ground structures," in *Proc. IEEE Topic. Meeting Silicon Monolithic Integr. Circuits RF Syst. (SiRF)*, New Orleans, LA, USA, Jan. 2010, pp. 92–95.

[12] Y.-L. Lai and P.-Y. Cheng, "CPW filters with defected ground structures for RF and microwave applications," in *Proc. Joint Conf. Inf. Sci.*, Kaohsiung, Taiwan, Oct. 2006, pp. 8–11.

[13] B. Pradhan and B. Gupta, "Ka-band tunable filter using metamaterials and RF MEMS varactors," *J. Mciroelectromech. Syst.*, vol. 24, no. 5, pp. 1453–1461, Oct. 2015.

[14] J.-S. Lim, C.-S. Kim, Y.-T. Lee, D. Ahn, and S. Nam, "A spiral-shaped defected ground structure for coplanar waveguide," *IEEE Microw. Wireless Compon. Lett.*, vol. 12, no. 9, pp. 330–332, Sep. 2002.

[15] S. Wang, W. Wang, E. Shin, T. Quach, and G. Subramanyam, "Tunable inductors using vanadium dioxide as the control material," *Microw. Opt. Techn. Lett.*, vol. 59, no. 5, pp. 1057–1061, May 2017.

[16] M. Fernández-Bolaños, J. Perruisseau-Carrier, P. Dainesi, and A. M. Ionescu, "RF MEMS capacitive switch on semi-suspended CPW using low-loss high-resistivity silicon substrate," *Microelectron. Eng.*, vol. 85, no. 6, pp. 1039–1042, Jun. 2008.

[17] X. Zuo and J. Yu, "A stepped-impedance bandstop filter with extended upper passbands and improved pass-band reflections," *AIP Adv.*, vol. 6, no. 9, pp. 1–6, Nov. 2016.

[18] W. A. Vitale *et al.*, "A steep-slope transistor combining phase-change and band-to-band-tunneling to achieve a sub-unity body factor," *Sci. Rep.*, vol. 7, no. 1, p. 355, 2017.

[19] A. A. Muller, P. Soto, D. Dascalu, D. Neculoiu, and V. E. Boria, "A 3-D smith chart based on the Riemann sphere for active and passive microwave circuits," *IEEE Microw. Compon. Lett.*, vol. 21, no. 6, pp. 286–288, Jun. 2011.

[20] A. A. Muller, E. Sanabria-Codesal, A. Moldoveanu, V. Asavei, and S. Lucyszyn, "Extended capabilities of the 3-D smith chart with group delay and resonator quality factor," *IEEE Trans. Microw. Theory Techn.*, vol. 65, no. 1, pp. 10–17, Jan. 2017.

[21] B. B. Mandelbrot, *The Fractal Geometry of Nature*. San Francisco, CA, USA: W. H. Freeman, 1982.

[22] A. Chakraborty and B. Gupta, "Development of compact 180° phase shifters based on MEMS technology," *Sens. Actuators A, Phys.*, vol. 247, pp. 187–198, Aug. 2016.

EMANUELE ANDREA CASU received the M.Sc. degree in micro and nano technologies for integrated systems jointly from Lausanne EPFL, Grenoble INP, and Politecnico di Torino in 2012. He is currently pursuing the Ph.D. degree with EPFL. His master's thesis was on oxides growth and characterization on graphene with the IBM Thomas J. Watson Research Center. In 2010, he had an undergraduate internship in a startup company, EULEGO srl, Turin, where he was focused on C programming for safety-critical embedded system. Since 2013, he has been with the Laboratory of Micro/Nanoelectronic Devices, EPFL, where he has been involved in MEMS resonators for communication and sensing applications, steep-slope switches based on insulator to metal transition, TMDC/VO_2 junctions, and reconfigurable RF functions based on VO_2.

ANDREI A. MÜLLER received the Ph.D. degree in telecommunications engineering from the University Politehnica of Bucharest in 2011. In 2012, he held a post-doctoral position with the Labsticc-CNRS Brest, France, with a focus on filter design. He received a four-year Marie Curie Integration Grant Fellowship, from the European Union, UPV Valencia, Spain, from 2013 to 2017. Since 2017, he has been with the Nanolab/EPFL, with a focus on microwave circuit design of smart materials. He received the Gheorghe Cartianu Award from the Romanian Academy for the 2011 *IEEE MWCL* article, A 3D Smith chart based on the Riemann Sphere for active and Passive Microwave Circuits, and launched in 2017 the first 3-D Smith chart tool. He has been an Associate Editor for the IEEE Access Journal since 2016.

MONTSERRAT FERNÁNDEZ-BOLAÑOS received the Ph.D. degree in microsystems and microelectronics from the École polytechnique fédérale de Lausanne (EPFL), Switzerland, in 2010. Since 2010, she has been a Scientific Collaborator, with the IBM Research Zurich, where she has been involved in NEM relay logic circuit for ultralow-power applications and also with the Swiss Federal Department of Defense, as a Research Project Manager in radars. She is currently a Senior Scientist and the Deputy of the Laboratory of Micro/Nanoelectronic Devices, EPFL. Her research interests include advanced materials and technologies for reconfigurable electronic devices including RF MEMS and metal-insulator transition vanadium dioxide. She has authored over 80 articles in international journals and conference proceeding. She is a member of the TPC Committee of IEDM and ESSDERC conferences since 2016.

ALESSANDRO FUMAROLA received the M.S. degree in nanotechnology jointly from the Polytechnic of Turin, INP Grenoble, and EPFL Lausanne. He is currently pursuing the Ph.D. degree with the Max Planck Institute for Microstructure Physics, Halle. He was with IBM Research-Almaden. His research interests include non-Von Neumann computing, phase-change materials, and magnetic microsystems.

ANNA KRAMMER received the M.Sc. degree in functional advanced materials and engineering jointly from INP Grenoble and TU Darmstadt. In 2015, she completed the master's thesis with the Solar Energy and Building Physics Laboratory, EPFL Lausanne, where she is currently pursuing the Ph.D. degree. Her Ph.D. topic was on thermochromic VO_2 based switchable absorber coatings for solar thermal applications.

ANDREAS SCHÜLER received the master's degree in physics from the University of Freiburg im Breisgau and the University of Michigan, Ann Arbor, and the Ph.D. degree from the University of Basel, with a focus on the electronic and optical properites of novel nanocomposite materials for solar selective absorber coatings. He started up a research group devoted to nanotechnology for solar energy conversion at the École polytechnique fédérale de Lausanne (EPFL). He is currently a Lecturer with EPFL and a Supervisor for Ph.D. and master's students. He was the Principal Organizer of the E-MRS Symposium on Carbon-Based Nanostructured Composite Films at the E-MRS Spring Meeting 2008, in Strasbourg, France, and received the Solar Energy Journal Best Technical Paper Award in 2007 and 2013.

ADRIAN M. IONESCU received the Ph.D. degree from the National Polytechnic Institute of Grenoble in France. He is currently a Full Professor with the Swiss Federal Institute of Technology, Lausanne (EPFL) in Switzerland. He has held staff and/or visiting positions with LETI-CEA, Grenoble, LPCS-ENSERG, and Stanford University from 1998 to 1999. He is the Director of the Laboratory of Micro/Nanoelectronic Devices (Nanolab), EPFL. He has authored over 250 articles in international journals and conference proceedings. His research interests include micro-and nanoelectronic devices aimed at integrated circuit design, particularly process development, modeling, and electrical characterization.